

The first crystal structure of a rhodium complex with the antileukaemic drug purine-6-thione; synthesis and molecular orbital investigation of new organorhodium(III) compounds ‡

Alessandro Cavaglioni and Renzo Cini*†

Department of Chemical and Biosystem Sciences and Technologies, University of Siena, Pian dei Mantellini 44, I-53100 Siena, Italy

Reactions of $[\text{Rh}^{\text{III}}\text{Cl}_2\text{Ph}(\text{SbPh}_3)_3]$ **1** with an excess of purine-6-thione ($\text{C}_5\text{H}_4\text{N}_4\text{S}$) or 1,3-thiazole ($\text{C}_3\text{H}_3\text{NS}$) in absolute ethanol gave crystalline $[\text{Rh}^{\text{III}}\text{Cl}_2\text{Ph}(\text{C}_5\text{H}_4\text{N}_4\text{S})(\text{SbPh}_3)_3]$ **2** (*S trans* to Sb), $[\text{Rh}^{\text{III}}\text{Cl}_2\text{Ph}(\text{SbPh}_3)(\text{C}_3\text{H}_3\text{NS})_2]$ **3** and $[\text{Rh}^{\text{III}}\text{Cl}_2\text{Ph}(\text{SbPh}_3)_2(\text{C}_3\text{H}_3\text{NS})]$ **4**. The crystal structure of complex **2** has been determined. Two different rotamers, which differ in the orientation of the phenyl ligand around the Rh–C bond axis, are present. The co-ordination geometry of both molecules is pseudo-octahedral and the neutral, N^1 and N^9 protonated, purine ligand behaves as bidentate through S and N^7 . The Rh– N^7 bonding interaction is much weakened [average 2.262(7) Å] by the high *trans* influence of the phenyl ligand. The H^8 atom of both purine systems points towards the centre of a phenyl ring of SbPh_3 . The geometrical parameters of the SbPh_3 molecules show that an attractive interaction between H^8 and the phenyl ring is operative for each rotamer. The ^1H NMR spectrum of **2**, in $\text{DCON}(\text{CD}_3)_2$, shows an upfield shift of 1.37 ppm for H^8 , consistent with a shielding effect from a phenyl ring of SbPh_3 . Therefore, the $\text{H}^8 \cdots \text{Ph}(\text{Sb})$ attractive interaction exists also in solution. The crystal structure of **3** has also been determined. The co-ordination geometry is pseudo-octahedral, the metal being linked to two *trans* chloride ions, one antimony donor from SbPh_3 , one carbon atom from the phenyl ligand and two nitrogen atoms from thiazole ligands, one of which is *trans* to Ph [Rh–N 2.245(5) Å]. The ^1H NMR spectrum shows that the solid-state structure is maintained in CDCl_3 solution. The signals of the H^2 and H^5 protons of the thiazole ligands are shifted downfield by 0.65 and 0.63 and 0.45 and 0.45 ppm for the molecules *trans* and *cis* to the C donor, respectively, upon complexation. The ^1H NMR spectrum of **4** is in agreement with the presence of a thiazole ligand *trans* to Ph. An interaction between the chloride ligands and some protons of the phenyl rings of SbPh_3 is responsible for a downfield chemical shift of about 0.2 ppm for the relevant ^1H NMR signals in compounds **1–4**. Molecular mechanics analysis based on the crystal structures of **2** and **3** made it possible to set up force-field parameters suitable for this class of molecules. In the case of **3** the rotation of the SbPh_3 molecule around the Rh–Sb bond is highly hindered; the lowest barrier between minima is higher than 125 kJ mol^{-1} . The rotations of the thiazole ligands have minima consistent with the crystal structure.

The synthesis, structural characterization and pharmacological activity of metal complexes containing active drugs as ligands is a field of growing interest for inorganic, medicinal and pharmacological chemistry.¹ This interest comes from the well known activity of many metal complexes and organometallic compounds² and because the administration of metal salts together with active drugs often increases the activity of the drugs themselves.³ The bonding mode of metal complexes with nucleic acids, nucleobases and nucleotides is often crucial to define the drug activity and the regulation of gene expression.^{4–7} Some investigations on this field have taken into account organometallic compounds.^{8–10} It has been known for at least two decades that some compounds of Rh^{I} and Rh^{III} have anti-cancer and antibacterial activities^{2b,c,11} whereas thiopurines are used as antileukaemic drugs and many thiazole-containing compounds are active against many different illnesses in humans.¹² A few examples are: the antineoplastic drug bleomycin, the antiallergic drug tiroxamast, the antiviral and anti-tumour drug tiazofurin.¹² Moreover, drug analogues of the anti-biotic, -neoplastic and -viral oligopeptides distamycin and netropsin include thiotropsin which binds adenine bases of DNA *via* the thiazole system.¹³

Furthermore the co-ordination and organometallic chem-

istry of rhodium(III) is intensively investigated in other fields such as the reactivity with small molecules like CS_2 , SO_2 , O_2 and S_8 ,¹⁴ to search for new catalysts for the synthesis of organic compounds and to shed light on the catalytic mechanisms.^{15–18}

For these reasons the efforts to synthesize metal complexes of thiopurines and thiazole, and to isolate organorhodium compounds, have been continued in this laboratory. We report here on the synthesis and structural characterization of organorhodium(III) compounds containing thiopurine and thiazole, as obtained from $[\text{Rh}^{\text{III}}\text{Cl}_2\text{Ph}(\text{SbPh}_3)_3]$,¹⁹ an organometallic compound which was earlier prepared in this laboratory from the reaction of RhCl_3 and SbPh_3 .

Experimental

Materials

The compounds $\text{RhCl}_3 \cdot 3\text{H}_2\text{O}$ (Janssen or Aldrich), 1,3-thiazole ($\text{C}_3\text{H}_3\text{NS}$) and dichloromethane (Janssen), purine-6-thione ($\text{C}_5\text{H}_4\text{N}_4\text{S}$) (Aldrich), $\text{Ag}(\text{O}_3\text{SCF}_3)$ and triphenylstibine, SbPh_3 (Fluka), absolute ethanol and acetone (Erba), methanol and diethyl ether (Merck), and ethyl acetate (Riedel) were used without further purification.

Preparations

Dichloro(phenyl)tris(triphenylstibine)rhodium(III)-tetrachloroethene (1/1), $[\text{Rh}^{\text{III}}\text{Cl}_2\text{Ph}(\text{SbPh}_3)_3] \cdot \text{C}_2\text{Cl}_4$ **1** · C_2Cl_4 . This compound was prepared by following a modification of the procedure in ref. 19. A solution of triphenylstibine (2.820 g, 8

† E-Mail: cini@unisi.it

‡ Supplementary data available (No. SUP 57214, 11 pp.): molecular mechanics and molecular orbital parameters, NMR spectra and crystal packing diagrams. See Instructions for Authors, *J. Chem. Soc., Dalton Trans.*, 1997, Issue 1.

mmol) in EtOH (30 cm³) was added to a clear solution of RhCl₃·3H₂O (0.527 g, 2 mmol) in EtOH (10 cm³). The resulting suspension (a yellow-orange microcrystalline solid started to precipitate a few seconds after mixing) was refluxed, with stirring, for 3 h. The salt Ag(O₃SCF₃) (0.514 g, 2 mmol) dissolved in EtOH (10 cm³) was added, dropwise, to the suspension and the resulting mixture refluxed in the dark for 3 h. The suspension (yellow) was cooled to room temperature and after 2 h the yellow microcrystalline solid was filtered off, washed three times with EtOH, twice with Et₂O, and then air dried for 24 h in the dark. Compound **1** was separated from AgCl *via* extraction with CH₂Cl₂. A 1 g amount of the solid mixture was loaded into a cylinder of S&S blue-band filter-paper which was then mounted on a sintered glass filter (G3) of a Soxhlet-extraction apparatus. The complex was extracted by refluxing in CH₂Cl₂ (total volume 25 cm³) for at least 6 h. The dark orange solution was cooled to room temperature and then mixed with a solution of triphenylstibine (0.530 g, 1.5 mmol) and EtOH (30 cm³); a yellow crystalline solid precipitated. Part of the solvent was evaporated through gentle heating and small amounts of EtOH (less than 5 cm³) were added to maintain the total volume at 50 cm³. Evaporation of the solvent and addition of EtOH was continued until the boiling point of the mixture was about 78 °C (most CH₂Cl₂ was removed); then the suspension was refluxed. Small amounts of the mixture (both solid and liquid) were periodically withdrawn, mixed with CH₂Cl₂ to dissolve the precipitate and tested by TLC (SiO₂, eluent CH₂Cl₂). The reflux was stopped when only two species could be detected (yellow spot, **1**, *R_f* = 0.90; colourless UV-sensitive spot, SbPh₃, *R_f* = 0.95). The suspension was cooled to -10 °C for at least 2 h, the crystalline yellow precipitate was filtered off, washed three times with EtOH, twice with Et₂O and air dried. The solid was then recrystallized from C₂Cl₄-EtOH, filtered off, washed with EtOH and stored under vacuum at room temperature. Yield 80% (Found: C, 49.8; H, 3.35; Cl, 14.1. Calc. for C₆₂H₅₀-Cl₆RhSb₃: C, 50.45; H, 3.45; Cl, 14.4%).

Dichloro(phenyl)(purine-6-thione)(triphenylstibine)-rhodium(III)-ethanol (1/1), [Rh^{III}Cl₂(C₅H₄N₄S)Ph(SbPh₃)]·EtOH 2·EtOH. Purine-6-thione (272 mg, 1.6 mmol) was dissolved in EtOH (30 cm³, 40 °C) and compound **1**·C₂Cl₄ (700 mg, 0.52 mmol) was added. The resulting mixture was refluxed for 6 h with stirring; the yellow crystalline solid (thin needles) was filtered off from the warm solution (40 °C), washed three times with warm EtOH and twice with Et₂O and then air dried for 48 h. Yield 40% (Found: C, 46.0; H, 3.7; Cl, 8.95; N, 7.15; S, 4.05. Calc. for C₃₁H₃₀Cl₂N₄ORhSSb: C, 46.4; H, 3.75; Cl, 8.85; N, 7.0; S, 4.0%). Single crystals of **2**·0.5MeOH suitable for X-ray data collection were obtained by slow evaporation of a MeOH solution containing the pure complex and free purine-6-thione.

Dichloro(phenyl)bis(1,3-thiazole)(triphenylstibine)-rhodium(III), [Rh^{III}Cl₂Ph(SbPh₃)(C₃H₃NS)₂] **3.** A mixture of compound **1**·C₂Cl₄ (155 mg, 0.116 mmol), 1,3-thiazole (300 mg, 3.5 mmol) and EtOH (8 cm³) was refluxed, with stirring, for 2 h (after a few minutes all the solid dissolved and the solution became pale yellow) and then cooled to room temperature. A red-orange crystalline solid precipitated; it was filtered off, washed three times with EtOH, twice with Et₂O, air dried for 48 h and then stored under vacuum. Yield 50% (Found: C, 46.4; H, 3.4; Cl, 9.2; N, 4.05; S, 7.95. Calc. for C₃₀H₂₆Cl₂N₂RhS₂Sb: C, 46.55; H, 3.4; Cl, 9.15; N, 3.6; S, 8.3%). Single crystals suitable for X-ray diffraction analysis were obtained through slow evaporation of a solution of the pure complex in acetone.

Dichloro(phenyl)(thiazole)bis(triphenylstibine)rhodium(III), [Rh^{III}Cl₂Ph(SbPh₃)₂(C₃H₃NS)] **4.** The procedure was that used to prepare compound **3**, except the amount of thiazole was decreased to 150 mg (1.75 mmol). Yield 60% (Found: C, 51.15;

H, 3.25; N, 1.1. Calc. for C₄₅H₃₈Cl₂NRhSSb: C, 51.85; H, 3.65; N, 1.35%).

Crystallography

Complex 2·0.5MeOH. A well formed red prism (0.30 × 0.40 × 0.50 mm) was selected through the polarizing microscope and mounted on a glass fibre. Preliminary X-ray diffraction analyses performed *via* oscillation and Weissenberg techniques did not show the presence of any symmetry in all the photograms and allowed an estimation of the cell constants. Accurate cell constants were determined using a Siemens P4 automatic four-circle diffractometer and full-matrix least-squares refinement of the values of 58 carefully centred randomly selected reflections (4 < 2θ < 32°). Crystallographic data are reported in Table 1. The data, collected at 293 K, by using Mo-Kα graphite-monochromatized radiation (λ 0.710 73 Å), were corrected for Lorentz-polarization and absorption effects (ψ -scan technique based on the reflections 0 -1 -1, 2 3 3 and -2 0 6). The structure solution and refinement [based on *F*², space group *P* $\bar{1}$ (no. 2)] (mean |*E*² - 1| 0.933; 0.968 for centrosymmetric and 0.736 for non-centrosymmetric space group) were performed through Patterson, Fourier and full-matrix least-squares methods. The H atoms of the purine ligand for both molecules of the asymmetric unit were located through the Fourier-difference maps. All the other H atoms were set in calculated positions *via* the AFIX option of SHELXL 93.²⁰ In the last cycles of refinement the Sb, Rh, Cl, S, N and C atoms were treated anisotropically. All the H atoms were refined isotropically. The refinement converged to *R*1 = 0.0425, *wR*2 = 0.0857 over 7489 reflections with *I* > 2σ(*I*). The scattering factors were those of SHELXS 86²¹ and SHELXL 93. All the calculations were carried out on VAX 6610 and IBM PC 486 machines using SHELXS and PARST²² packages.

Complex 3. A well formed orange-red prism (0.40 × 0.50 × 0.60 mm) was selected at the polarizing microscope and mounted on a glass fibre. A preliminary X-ray diffraction investigation, carried out by oscillation and Weissenberg methods, gave approximate cell constants for the *P*₂₁/*n* (no. 14) space group. The accurate cell constant determination (and full data collection) was carried out as above on the basis of the values for the angles of 33 randomly selected reflections in the range 9 < 2θ < 40° analysed *via* full-matrix least squares. The data were collected and the intensities were corrected as above (absorption based on the reflections 1 3 4, 0 4 4 and 3 10 9). The structure solution and refinement (space group *P*₂₁/*n*, from systematic absences; mean |*E*² - 1| 0.931) were also performed as above. The Fourier-difference synthesis after eight cycles at the isotropic level showed peaks higher than 1 e Å⁻³ near atoms C(42) and S(2) of one of the thiazole ligands (the thermal parameters of the two atoms were relatively very high). These were interpreted as due to a statistical disorder of the thiazole molecule around the Rh-N(2) axis. Two new atoms, C(42B) and S(2B), were then assigned to the extra peaks and included in the final refinement. Atoms C(42), S(2), C(42B) and S(2B) were treated isotropically, whereas the site occupancy factors (s.o.f.s) were refined by imposing the conditions: s.o.f. [C(42)] = s.o.f. [S(2)]; s.o.f. [C(42B)] = s.o.f. [S(2B)]; s.o.f. {C(42)[S(2)]} + s.o.f. {C(42B)[S(2B)]} = 1. The bond distances C(22)-S(2), C(42)-S(2), C(42B)-S(2B) and C(52)-S(2B) were fixed at 1.70(3) Å, C(22)-C(42B) and C(42)-C(52) at 1.33(3) Å. The N(1)C(21)S(1)C(41)C(51) thiazole ligand is not affected by disorder analogous to that described above, even though the bond distances C(41)-C(51) and C(41)-S(1) had to be fixed at 1.33(3) and 1.70(3) Å, respectively. In the last cycles of refinement the Sb, Rh, Cl, S, N and all C atoms, except C(42) and C(42B), were considered anisotropic. As the Fourier-difference map was not able to show the positions of all the H atoms, these were set at calculated positions [H(42) was not located because of the disorder] through the AFIX option of SHELXL 93. The

refinement converged to $R1 = 0.0406$ and $wR2 = 0.0991$. The scattering factors were those of SHELXL 93 and SHELXS 86 and of ref. 23. The isotropic thermal parameters for the H atoms of Ph, for H(51) and H(21), and for H(52) and H(22), were refined to 0.062(9), 0.098(22), 0.089(18) Å², respectively. The U parameter for the H atoms of triphenylstibine was tied at 1.2 $U(\text{eq})$ of the relative carbon atom. Computers and packages were those for 2·0.5MeOH.

Atomic coordinates, thermal parameters, bond lengths and angles have been deposited at the Cambridge Crystallographic Data Centre (CCDC). See Instructions for Authors, *J. Chem. Soc., Dalton Trans.*, 1997, Issue 1. Any request to the CCDC for this material should quote the full literature citation and the reference number 186/396.

Spectroscopy

The IR spectra, in the range 4000–200 cm⁻¹, were recorded *via* the KBr pellet technique on a Perkin-Elmer model 1600 Fourier-transform spectrometer, ¹H NMR spectra on a Bruker AC-200 spectrometer.

Molecular orbital calculations

Extended-Hückel (EH) type molecular-orbital calculations were carried out by the ICONC&INPUTC package²⁴ implemented on a VAX 6610 computer. The parameters used were those standard in the program. The distance-dependent weighted Wolfsberg–Helmholz formula (see documentation for ICONC&INPUTC) was applied. In order to simplify the analysis, the stibine molecule was substituted for triphenylstibine. The models were built from experimental solid-state geometries using the molecular graphics package MACROMODEL 3.0²⁵ (graphic output *via* an Evans&Sutherland PS390 machine). The geometry of the molecules was kept fixed for all the calculations. The axis set was approximately as follows: x , Rh–N(7); y , Rh–Sb; z , Rh–Cl(1) for complex **2**; x , Rh–C(1); y , Rh–N(2); z , Rh–Cl(2) for **3**.

Molecular mechanics calculations

The strain energies of the metal complexes were computed as the sum $E_{\text{tot}} = E_b + E_0 + E_\phi + E_{\text{nb}} + E_{\text{hb}}$ (bond-length deformation, valence-angle deformation, torsion-angle deformation, non-bonding interaction, hydrogen-bonding interaction, respectively). The force field used was AMBER²⁶ implemented in MACROMODEL 3.0.²⁵ Modification and extension of the force field was carried out in order to model the co-ordination sphere. The force field parameters were obtained *via* a trial-and-error procedure which gave excellent agreement between calculated and observed structures. The force fields used in this study are given in Table 5. They are in acceptable agreement with those previously reported in molecular mechanics studies for other metal complexes and organometallic compounds (see ref. 27 and refs. therein). The total energy (E_{tot}) was minimized *via* the block-diagonal matrix Newton–Raphson method until the root-mean-square value of the first derivative vector was less than 0.01 kJ Å⁻¹. The starting structures were those found *via* single crystal X-ray diffraction for **2** and **3**. The calculations were carried out by using the MACROMODEL 3.0 package implemented on a VAX 6610 computer.

Results and Discussion

Structure of [Rh^{III}Cl₂(C₅H₄N₄S)Ph(SbPh₃)₃] \cdot 0.5MeOH 2 \cdot 0.5MeOH

The bond lengths and angles are listed in Table 2. Two distinct complex molecules are present in the asymmetric unit [Fig. 1(a)]; a superimposition of the two is pictured in Fig. 1(b). The two molecules differ in the orientation of the Ph ligand and the phenyl groups of SbPh₃ when the Rh, Sb, Cl, S and N⁷ atoms are superimposed.

Table 1 Crystal data and structure refinement^a for [RhCl₂Ph(C₅H₄N₄S)(SbPh₃)₃] \cdot 0.5MeOH, 2 \cdot 0.5MeOH and [RhCl₂Ph(SbPh₃)(C₃H₃NS)₂]**3**

	2	3
Empirical formula	C _{29.5} H ₂₆ Cl ₂ N ₄ O _{0.5} RhSSb	C ₃₀ H ₂₆ Cl ₂ N ₂ RhS ₂ Sb
M	772.16	774.21
Space group	$P\bar{1}$ (no. 2)	$P2_1/n$ (no. 14)
Crystal system	Triclinic	Monoclinic
$a/\text{Å}$	11.0360(10)	9.800(2)
$b/\text{Å}$	15.4960(10)	28.046(6)
$c/\text{Å}$	18.922(2)	11.095(6)
$\alpha/^\circ$	113.350(10)	
$\beta/^\circ$	92.740(10)	97.00(3)
$\gamma/^\circ$	93.320(10)	
$U/\text{Å}^3$	2957.1(5)	3027(2)
$D_x/\text{Mg m}^{-3}$	1.734	1.699
μ/mm^{-1}	1.751	1.775
$F(000)$	1524	1528
Data, restraints, parameters	7489, 0, 731	4428, 8, 358
Final $R1, wR2^b$ [$I > 2\sigma(I)$]	0.0425, 0.0857	0.0406, 0.0991
(all data)	0.0764, 0.1073	0.0573, 0.1122

^a Details in common: 293(2) K; $Z = 4$. ^b Weighting scheme as in ref. 20.

The co-ordination sphere. The rhodium(III) ions have a pseudo-octahedral co-ordination geometry: two chloride anions are *trans* to each other (axial positions) and a carbon atom from Ph and an antimony atom from a triphenylstibine ligand occupy two *cis* equatorial positions. The purine ligand behaves as bidentate through S⁶ and N⁷ (the latter is *trans* to Ph). The Rh–Cl bond distances average 2.364(2) Å and are in agreement with the mean value of 2.354(2) Å found for [RhCl₂Ph(SbPh₃)₃], [RhCl₂Ph(py)₃] (py = pyridine), [RhCl₂Ph(dmpy)₃]¹⁹ (dmpy = 3,5-dimethylpyridine) and [RhCl₂Ph(NCMe)(SbPh₃)₂]²⁸ Other Rh^{III}–Cl bond distances are 2.333(1) Å (average) for *trans*-[Rh^{III}Cl₂(Hpz-N²)₄]⁺ (Hpz = pyrazole),²⁹ 2.337(4) (average) for *mer*-[Rh^{III}Cl₃(py)₃],³⁰ 2.302(3) (*trans* to N) and 2.436(3) Å (*trans* to P) for [Rh^{III}Cl₃(dppm)(NCMe)] (dppm = Ph₂PCH₂PPh₂),³¹ 2.34(1) (*trans* to Cl) and 2.43(1) Å (*trans* to P) for [Rh^{III}Cl₃(dppm)(PBuⁿ)₃].³¹

The Rh–Sb bond (*trans* to S) distances, average 2.5550(9) Å, can be compared with the means of 2.588(2) and 2.588(1) Å found for the two stibines (*trans* to each other) of [RhCl₂Ph(SbPh₃)₃]¹⁹ and [RhCl₂Ph(NCMe)(SbPh₃)₂]²⁸ [the difference is about 15 times larger than the estimated standard deviations (e.s.d.s) and can be due to both a higher steric hindrance in the complexes which contain more than one triphenylstibine molecule and to a larger *trans* influence of Sb when compared with that of S]. The Rh–C bond distances average 2.033(9) Å and are in agreement with the mean found for [RhCl₂Ph(NCMe)(SbPh₃)₂] [2.044(10) Å].²⁸ The value [2.09(2) Å] for [RhCl₂Ph(SbPh₃)₃] seems to be higher and can be explained on the basis of a relatively large *trans* influence of Sb when compared to that of N. The present Rh–C distances are in agreement also with those of 1.992(3) and 1.989(5) Å found for [Rh^{III}L₂(bipy)]⁺ [bipy = 2,2'-bipyridine, HL = 2-phenylpyridine³² or 2-(2-thienyl)pyridine³³] respectively. The Rh–S bond lengths [average 2.403(2) Å] are somewhat shorter than the Ru^{II}–S distances [average 2.432(4) Å] found for [Ru(C₅H₄N₄S)₂(PPh₃)₂]^{2+ 34} and [Ru^{II}(Htpr)₂(PPh₃)₂]²⁺ (Htpr = ribosylpurine-6-thione),³⁵ Rh^{III}–S bond lengths for [Rh^{III}(NC₅H₄SH-2)₂(NC₅H₄S)]⁺ are 2.360(4) (thiolate) and 2.375(4) Å (thiol),³⁶ respectively. The Rh–N bond distances [average 2.262(7) Å] are much longer than the Rh–N (CMe) distance [2.163(9) Å] of [Rh^{III}Cl₂Ph(NCMe)(SbPh₃)₂]²⁸ and than the Rh–N (py) distance of [Rh^{III}(NC₅H₄Ph)₂(bipy)]⁺^{32,33} [2.039(2), N *cis* to C; 2.142(2) Å, N *trans* to C], and much longer than all the M–N values found for S⁶, N⁷ chelating purine-6-thione in mononuclear complexes of platinum-group metal ions. The Ru–N⁷ distances found for

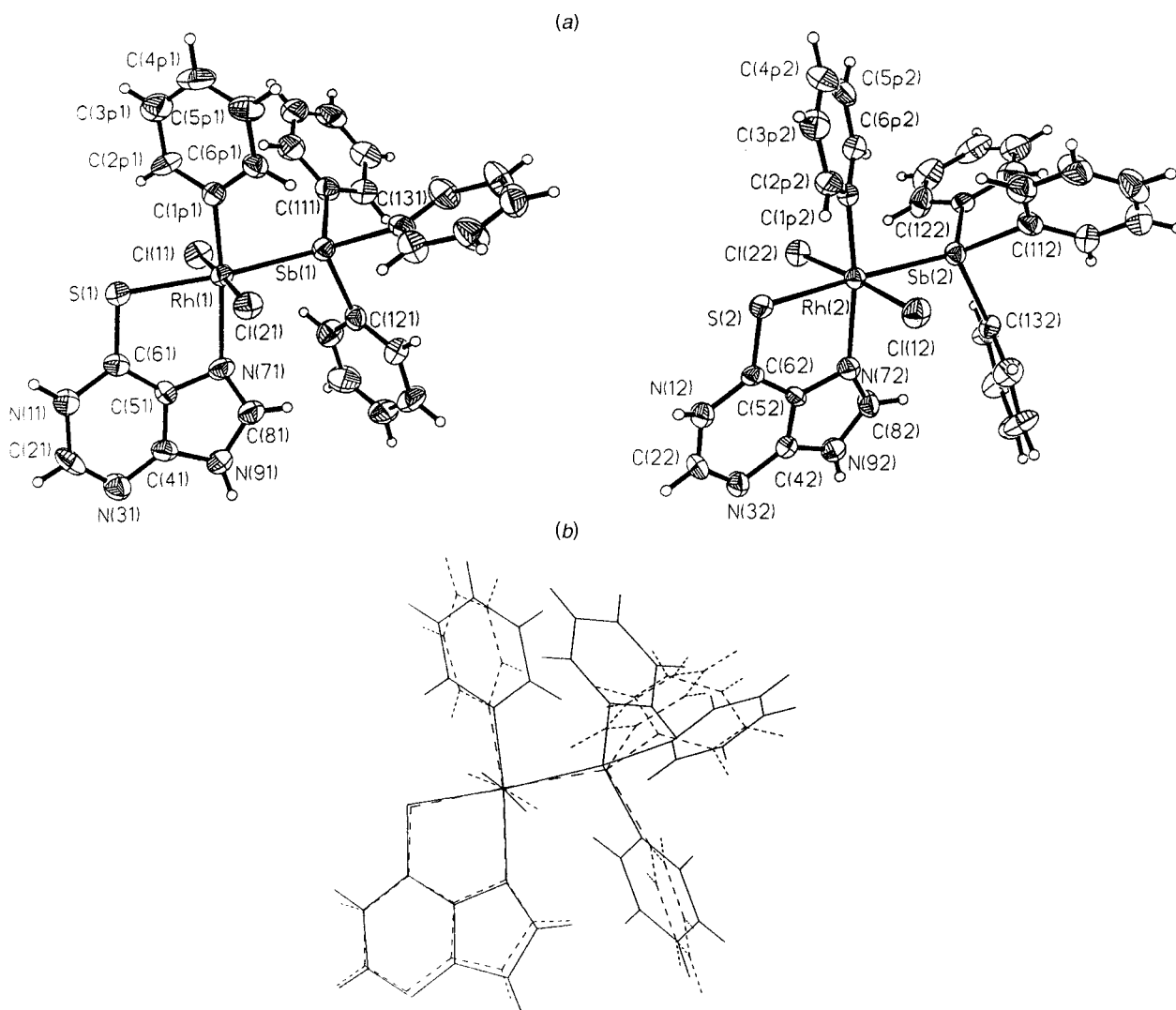
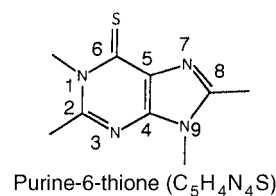


Fig. 1 (a) The two molecules of complex **2** with the labelling scheme. Ellipsoids enclose 30% probability. (b) Superimposition of the two molecules

$[\text{Ru}^{\text{II}}(\text{Htpr})_2(\text{PPh}_3)_2]^{2+}$ ³⁵ and $[\text{Ru}^{\text{II}}(\text{C}_5\text{H}_4\text{N}_4\text{S})_2(\text{PPh}_3)_2]^{2+}$ ³⁴ are 2.15(1) and 2.10(1) Å, respectively. Other Rh^{III}–N bond lengths are 2.06(1) Å (average) for *mer*- $[\text{Rh}^{\text{III}}\text{Cl}_3(\text{py})_3]$,³⁰ 2.038(3) Å (average) for *trans*- $[\text{Rh}^{\text{III}}\text{Cl}_2(\text{Hpz}-\text{N}^2)_4]^+$,²⁹ and 2.070(8) Å (average) for *trans*- $[\text{Rh}^{\text{III}}\text{Br}_2(\text{py})_4]^+$.³⁷ The high *trans* influence of the phenyl ligand explains in part the long Rh–N⁷ bond distance found for **2**.

The bond angles around Rh have significant deviations from the idealized values, the largest one being found for S(1)–Rh(1)–Sb(1) [170.93(6)°].

The purine ligand. The S⁶/N⁷ intramolecular bite distances [average 3.144(7) Å] are longer than the values found for complexes of Ru^{II} and Pd^{II} [3.10(1)³⁴ and 3.05(1) Å,³⁸ respectively], in agreement with a decrease in the Rh^{III}–N⁷ bond strength when compared to those of Ru^{II}– and Pd^{II}–N⁷. The purine ligands of both molecules of the asymmetric unit are protonated on N¹ and N⁹; all the four H atoms of each purine were located through the Fourier-difference syntheses and their positions refined through least-squares cycles. The N⁹–C⁴–C⁵ and C⁴–C⁵–N⁷ bond angles are 105.2(8) and 105.1(8) and 110.7(8) and 110.7(7)° for the two molecules respectively, in agreement with the protonation on N⁹ (see ref. 39). The protonation of N¹ of both purines is consistent with the values of the C²–N¹–C⁶ bond angles [121.3(9) and 122.2(8)°] on the basis of the Singh rule⁴⁰ (125 ± 3° for N¹ protonated, and 116 ± 3° for non-protonated purine bases). The protonation status of N¹ is also in agreement with the values of C²–N¹–C⁶ found for the anionic and neutral purine-6-thione ligands in recent works: 115.4(3)° for [Co^{III}–



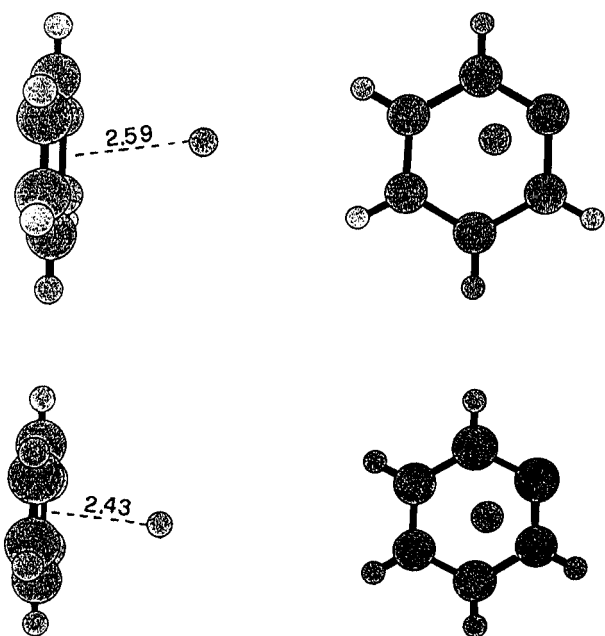
(C₅H₂N₄S)(en)₂)⁺ (en = ethane-1,2-diamine)^{41a} and 124.3(1)° for [Cd^{II}(C₅H₄N₄S)₂Cl₂].^{41b}

The C⁶–S bond distances [average 1.685(8) Å] are significantly shorter than the C–S bond distance typical of a SH group (1.80–1.85 Å^{41a,42}). The analysis of the pyrimidine system bond lengths [N¹–C² 1.382(13), N¹–C⁶ 1.369(13), C²–N³ 1.289(13), N³–C⁴ 1.347(14), C⁴–C⁵ 1.372(12), C⁵–C⁶ 1.382(11) Å] also indicates that the ligand molecule has a ‘thio’ instead of a ‘mercapto’ form. The purine systems of both molecules are almost coplanar, the largest deviation from the least-squares planes being that of C(51) [0.063(8) Å]. It is noteworthy that the metal centres deviate significantly from the purine planes [average 0.1618(7) Å]. The Rh–N⁷–C⁸, Rh–N⁷–C⁵ and C⁵–N⁷–C⁸ angles average 148.1(7), 107.7(5) and 103.6(7)°, respectively. The Rh–N⁷–C⁵ angle found for $[\text{Ru}^{\text{II}}(\text{Htpr})_2(\text{PPh}_3)_2]^{2+}$ and $[\text{Ru}^{\text{II}}(\text{C}_5\text{H}_4\text{N}_4\text{S})_2(\text{PPh}_3)_2]^{2+}$ are 112(1)³⁵ (average of four values) and 111(1)°³⁴ (average of two values), respectively.

Of interest is the fact that in both molecules the chelate purine system is almost perpendicular to the plane of a phenyl ring of triphenylstibine [see Fig. 1; dihedral angles: 109.9(2)°, purine 1/C(121)–C(621); 71.3(2)°, purine 2/C(132)–C(632)].

Table 2 Selected bond lengths (Å) and angles (°) for complex **2**·0.5MeOH

Rh(1)–C(1p1)	2.029(8)	Rh(2)–S(2)	2.407(2)	N(11)–C(61)	1.374(10)	N(72)–C(82)	1.294(10)
Rh(1)–N(71)	2.275(7)	Rh(2)–Sb(2)	2.5576(9)	N(11)–C(21)	1.387(12)	N(72)–C(52)	1.390(10)
Rh(1)–Cl(11)	2.337(2)	Sb(1)–C(111)	2.130(8)	N(12)–C(62)	1.364(10)	N(91)–C(81)	1.350(12)
Rh(1)–Cl(21)	2.395(2)	Sb(1)–C(121)	2.139(8)	N(12)–C(22)	1.378(12)	N(91)–C(41)	1.368(11)
Rh(1)–S(1)	2.400(2)	Sb(1)–C(131)	2.155(9)	N(31)–C(21)	1.288(12)	N(92)–C(82)	1.352(11)
Rh(1)–Sb(1)	2.5525(9)	Sb(2)–C(132)	2.127(8)	N(31)–C(41)	1.343(11)	N(92)–C(42)	1.357(11)
Rh(2)–C(1p2)	2.037(8)	Sb(2)–C(112)	2.132(8)	N(32)–C(22)	1.292(11)	C(41)–C(51)	1.376(11)
Rh(2)–N(72)	2.250(7)	Sb(2)–C(122)	2.140(8)	N(32)–C(42)	1.352(10)	C(42)–C(52)	1.368(11)
Rh(2)–Cl(12)	2.343(2)	S(1)–C(61)	1.681(8)	N(71)–C(81)	1.312(11)	C(51)–C(61)	1.377(11)
Rh(2)–Cl(22)	2.381(2)	S(2)–C(62)	1.690(8)	N(71)–C(51)	1.386(10)	C(52)–C(62)	1.386(11)
C(1p1)–Rh(1)–N(71)	172.8(3)	C(1p2)–Rh(2)–S(2)	88.2(2)	C(61)–S(1)–Rh(1)	97.8(3)	N(31)–C(41)–N(91)	129.1(8)
C(1p1)–Rh(1)–Cl(11)	94.2(2)	N(72)–Rh(2)–S(2)	85.0(2)	C(62)–S(2)–Rh(2)	97.3(3)	N(31)–C(41)–C(51)	125.7(8)
N(71)–Rh(1)–Cl(11)	89.1(2)	Cl(12)–Rh(2)–S(2)	89.61(8)	C(61)–N(11)–C(21)	121.4(8)	N(91)–C(41)–C(51)	105.2(8)
C(1p1)–Rh(1)–Cl(21)	88.9(2)	Cl(22)–Rh(2)–S(2)	90.02(8)	C(62)–N(12)–C(22)	122.2(7)	N(32)–C(42)–N(92)	129.3(8)
N(71)–Rh(1)–Cl(21)	87.7(2)	C(1p2)–Rh(2)–Sb(2)	91.7(2)	C(21)–N(31)–C(41)	112.0(8)	N(32)–C(42)–C(52)	125.4(8)
Cl(11)–Rh(1)–Cl(21)	176.76(9)	N(72)–Rh(2)–Sb(2)	95.6(2)	C(22)–N(32)–C(42)	111.9(7)	N(92)–C(42)–C(52)	105.2(7)
C(1p1)–Rh(1)–S(1)	89.3(2)	Cl(12)–Rh(2)–Sb(2)	82.97(6)	C(81)–N(71)–C(51)	103.7(7)	C(41)–C(51)–C(61)	121.4(8)
N(71)–Rh(1)–S(1)	84.4(2)	Cl(22)–Rh(2)–Sb(2)	97.42(6)	C(81)–N(71)–Rh(1)	147.9(7)	C(41)–C(51)–N(71)	110.7(8)
Cl(11)–Rh(1)–S(1)	88.30(8)	S(2)–Rh(2)–Sb(2)	172.56(6)	C(51)–N(71)–Rh(1)	107.7(5)	C(61)–C(51)–N(71)	127.7(8)
Cl(21)–Rh(1)–S(1)	90.89(8)	C(111)–Sb(1)–C(121)	103.4(3)	C(82)–N(72)–C(52)	103.5(7)	C(42)–C(52)–C(62)	121.5(7)
C(1p1)–Rh(1)–Sb(1)	88.8(2)	C(111)–Sb(1)–C(131)	99.7(3)	C(82)–N(72)–Rh(2)	148.3(6)	C(42)–C(52)–N(72)	110.7(7)
N(71)–Rh(1)–Sb(1)	98.0(2)	C(121)–Sb(1)–C(131)	98.2(3)	C(52)–N(72)–Rh(2)	107.8(5)	C(62)–C(52)–N(72)	127.7(7)
Cl(11)–Rh(1)–Sb(1)	83.00(6)	C(111)–Sb(1)–Rh(1)	116.7(2)	C(81)–N(91)–C(41)	106.9(8)	N(11)–C(61)–C(51)	112.7(7)
Cl(21)–Rh(1)–Sb(1)	97.94(6)	C(121)–Sb(1)–Rh(1)	109.3(2)	C(82)–N(92)–C(42)	106.8(7)	N(11)–C(61)–S(1)	124.9(7)
S(1)–Rh(1)–Sb(1)	170.93(6)	C(131)–Sb(1)–Rh(1)	126.0(2)	C(2p1)–C(1p1)–Rh(1)	120.0(6)	C(51)–C(61)–S(1)	122.3(7)
C(1p2)–Rh(2)–N(72)	171.8(3)	C(132)–Sb(2)–C(112)	100.1(3)	C(6p1)–C(1p1)–Rh(1)	122.8(6)	N(12)–C(62)–C(52)	112.3(7)
C(1p2)–Rh(2)–Cl(12)	94.3(2)	C(132)–Sb(2)–C(122)	98.8(3)	C(2p2)–C(1p2)–Rh(2)	120.4(6)	N(12)–C(62)–S(2)	125.8(6)
N(72)–Rh(2)–Cl(12)	90.2(2)	C(112)–Sb(2)–C(122)	101.6(3)	C(6p2)–C(1p2)–Rh(2)	122.4(6)	C(52)–C(62)–S(2)	121.9(6)
C(1p2)–Rh(2)–Cl(22)	90.0(2)	C(132)–Sb(2)–Rh(2)	109.8(2)	N(31)–C(21)–N(11)	126.8(9)	N(71)–C(81)–N(91)	113.4(8)
N(72)–Rh(2)–Cl(22)	85.5(2)	C(112)–Sb(2)–Rh(2)	118.7(2)	N(32)–C(22)–N(12)	126.6(8)	N(72)–C(82)–N(92)	113.7(8)
Cl(12)–Rh(2)–Cl(22)	175.71(8)	C(122)–Sb(2)–Rh(2)	123.8(2)				

**Fig. 2** Diagrams showing the interactions of H⁸ and a phenyl ring of SbPh₃ for the two molecules of complex **2**. Distances in Å

Furthermore, atom H⁸ points towards the centre of the aromatic ring (Fig. 2) from which it is separated by 2.59 and 2.43 Å, for the two molecules respectively. This suggests that an attractive intramolecular interaction exists between the positively charged proton H⁸ and the π -electronic cloud (see below, spectroscopy). The analysis of the geometrical parameters confirms this expectation; the Rh–Sb–C angle for the phenyl group involved in this interaction is 109.5(2)° (average), whereas the other two Rh–Sb–C angles are in the range 116.7(2)–126.0(2)°. The angles between the Sb–C direction and the normal to the phenyl planes average 9°, in favour of a bonding interaction between H⁸ and a phenyl ring. Hydrogen bonds

between H⁸ and oxygen atoms at the ribose O(5') position are common for nucleosides and nucleotides;⁴³ however, to our knowledge the type of interaction found in this work has never been described for purine–metal complexes.

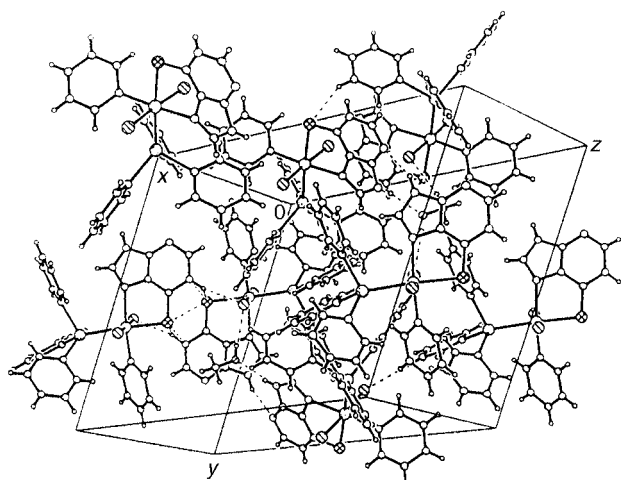
The phenyl ligand. The phenyl ligand atoms are also coplanar, the largest deviation being that of C(5p2) [0.020(1) Å, SUP 57214], whereas the rhodium centres deviate [0.1214(7) and 0.2310(7) Å] significantly from the phenyl ligand planes which are staggered with respect to the Rh–Cl axes. The absolute values of the Cl–Rh–C–C torsion angles are 43.7(7) and 43.5(7)°. Values of 13.8(5), 34.3(7), 41.9(5) and 44.8(5)° were found for the corresponding torsion angles of [RhCl₂Ph(SbPh₃)₃], [RhCl₂Ph(NCMe)(SbPh₃)₂], [RhCl₂Ph(py)₃] and [RhCl₂Ph(dmpy)₃], respectively. Some more information on the geometry of the Ph ligand is given below (see description of compound **3**).

The triphenylstibine ligand. The six Sb–C bond lengths are in the range 2.127(8)–2.155(9) Å [average 2.137(8) Å] in agreement with those of 2.12(2)–2.17(2) [2.14(2) Å], 2.135(2)–2.121(2) [2.128(2) Å] and 2.130(3)–2.190(3) [2.158(3) Å] found for [RhCl₂Ph(SbPh₃)₃], [RhCl₂Ph(NCMe)(SbPh₃)₂] and *trans*-[Ru^{II}Cl₂(SbPh₃)₄].⁴⁴ The Sb atoms of both molecules have a distorted-tetrahedral geometry, the Rh–Sb–C bond angles spanning a wide range, 109.3(2)–126.0(2)°. However, the C–Sb–C bond angles fall within a narrow range, 98.1(3)–103.4(3)° [average 100.3(3)°, SUP 57214], in agreement with the values found for [RhCl₂Ph(SbPh₃)₃] [98.7(8)°], [RhCl₂Ph(NCMe)(SbPh₃)₂] [100.5(3)°], [Rh^{III}LPh₂(SbPh₃)₂] (L = 1,3-diphenylpropane-1,3-dione) [101.0°],⁴⁵ and *trans*-[Ru^{II}Cl₂(SbPh₃)₄] [92.8(2)–102.4(2)°].⁴⁴

Crystal packing. The analysis of the crystal packing (Fig. 3) shows that there is an extensive network of hydrogen bonds involving the nitrogen atoms of the purine systems, the methanol molecule and the chloride ligands. The oxygen atom of methanol [O(M)] is linked to the purine N(92) atom [O(M)⋯N(92) (−x + 1, −y + 1, −z + 1) 2.71(1) Å; O(M)⋯

Table 3 Selected bond lengths (Å) and angles for complex **3**

Rh–C(1)	2.037(6)	N(1)–C(51)	1.377(9)
Rh–N(2)	2.120(5)	N(2)–C(22)	1.319(8)
Rh–N(1)	2.245(5)	N(2)–C(52)	1.345(8)
Rh–Cl(1)	2.344(2)	C(1)–C(2)	1.387(8)
Rh–Cl(2)	2.363(2)	C(1)–C(6)	1.394(8)
Rh–Sb	2.5324(7)	C(2)–C(3)	1.390(9)
S(1)–C(41)	1.642(8)	C(3)–C(4)	1.374(11)
S(1)–C(21)	1.704(8)	C(4)–C(5)	1.357(10)
S(2)–C(22)	1.622(10)	C(5)–C(6)	1.382(9)
S(2)–C(42)	1.71(2)	C(41)–C(51)	1.415(10)
C(42B)–C(22)	1.38(3)	S(2B)–C(52)	1.681(10)
C(42B)–S(2B)	1.72(3)	C(42)–C(52)	1.36(2)
N(1)–C(21)	1.307(9)		
C(1)–Rh–N(2)	87.5(2)	C(41)–S(1)–C(21)	93.7(4)
C(1)–Rh–N(1)	178.4(2)	C(22)–S(2)–C(42)	91.4(9)
N(2)–Rh–N(1)	91.3(2)	C(22)–C(42B)–S(2B)	107(2)
C(1)–Rh–Cl(1)	91.0(2)	C(21)–N(1)–C(51)	109.8(6)
N(2)–Rh–Cl(1)	89.95(14)	C(22)–N(2)–C(52)	109.6(6)
N(1)–Rh–Cl(1)	87.9(2)	N(1)–C(21)–S(1)	113.3(7)
C(1)–Rh–Cl(2)	93.1(2)	C(51)–C(41)–S(1)	107.1(6)
N(2)–Rh–Cl(2)	91.86(14)	N(1)–C(51)–C(41)	116.1(7)
N(1)–Rh–Cl(2)	88.0(2)	N(2)–C(22)–C(42B)	117.9(14)
Cl(1)–Rh–Cl(2)	175.58(6)	N(2)–C(22)–S(2)	115.7(6)
C(1)–Rh–Sb	86.5(2)	C(52)–S(2B)–C(42B)	90.5(11)
N(2)–Rh–Sb	173.25(14)	C(52)–C(42)–S(2)	107(2)
N(1)–Rh–Sb	94.7(2)	N(2)–C(52)–C(42)	116.2(13)
Cl(1)–Rh–Sb	93.22(5)	N(2)–C(52)–S(2B)	114.7(5)
Cl(2)–Rh–Sb	85.41(5)		

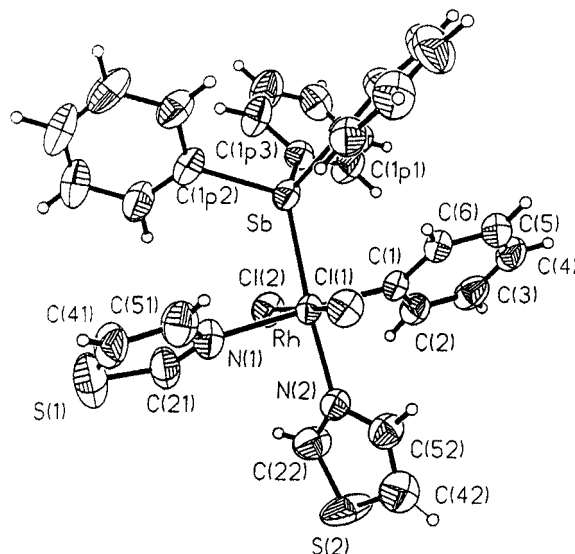
**Fig. 3** View of the crystal packing of complex **2**·0.5MeOH

H–N(92) 167°]. Purine N(11) is linked to a chloride ligand [Cl(21)⋯N(11) (–*x* + 1, –*y* + 1, –*z*) 3.298(8) Å; Cl(21)⋯H–N(11) 166°], whereas N(91) interestingly donates to N(32) [N(91)⋯N(32) (–*x* + 1, –*y* + 1, –*z* + 1) 3.145(9) Å; N(91)–H⋯N(32) 147°]. No significant inter- and intra-molecular stacking interactions could be found in the crystal. A more detailed analysis of the packing did not reveal any force which could bring the H⁸ atom in short contact with a SbPh₃ aromatic ring.

Structure of [Rh^{III}Cl₂Ph(SbPh₃)(C₃H₃NS)₂]**3**

The bond lengths and angles are listed in Table 3, whereas the drawing of the complex molecule is in Fig. 4.

The co-ordination sphere. The co-ordination sphere geometry is pseudo-octahedral. Two *trans* positions are occupied by chloride ions, one of the equatorial position by a carbon atom of Ph, a second by the antimony atom and the remaining two are saturated by the nitrogen atoms (*cis* to each other) of two thiazole molecules. The Rh–Cl, Rh–Sb and Rh–C bond distances 2.348(2) (average), 2.5324(7) and 2.037(6) Å are in excel-

**Fig. 4** Structure of complex **3** with the atom labelling (30% probability); H(42) was not included in the calculations

lent agreement with the values reported above for the purine derivative: the Rh–N bond lengths differ more than 20 times the e.s.d.s; the Rh–N(1) vector [2.245(5) Å] is *trans* to C (Ph) and experiences a weakening influence larger than that caused by Sb on Rh–N(2) [2.120(5) Å]. The co-ordination-sphere bond angles are close to idealised values, the minimum value being that of Sb–Rh–Cl(2) [85.41(5)°] and the maximum that of Sb–Rh–N(1) [94.7(2)°].

The phenyl ligand. The high accuracy of the crystal structure determination for complexes **2** and **3** allows the discrimination of some subtle but significant geometrical effects on the Ph ligand. The pairs of vectors C(1)–C(2) and C(1)–C(6), C(2)–C(3) and C(5)–C(6), C(3)–C(4) and C(4)–C(5) average 1.390 and 1.395, 1.386 and 1.385, and 1.365 and 1.373 Å, for **2** and **3**, respectively. The trend is the same in the two crystal structures, so the C–C vectors far from the Rh–C bond [C(3)–C(4) and C(4)–C(5)] are shorter than the closer one. Bond angles relevant to the Rh–C₆H₅ group range from 123.0(4) [Rh–C(1)–C(6)] to 116.8(5)° [C(2)–C(1)–C(6)]: the inner angle on the donor atom is the smallest one. The metal centre deviates 0.0510(6) Å from the phenyl plane.

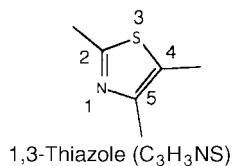
The thiazole ligand. The geometrical parameters for the thiazole systems can be analysed in detail only for the N(1)C(21)S(1)C(41)C(51) ring thiazole 1, as the thiazole 2 ligand has relatively high e.s.d.s because of statistical disorder. This disorder arises from the possibility of two different orientations of the approaching ligand when one of the triphenylstibine molecules *cis* to Ph is removed. The insertion of the first thiazole ligand is much more hindered and just one orientation is allowed. Thermal disorder is ruled out by the high barriers to rotations around the Rh–N and Rh–C bonds (see below, molecular mechanics, for an interpretation of disorder for thiazole 2).

The N(1)–C(21) bond length [1.307(9) Å] is much shorter than N(1)–C(51) [1.377(9) Å] consistent with the form shown. However, some delocalization of the π electrons must occur as N(1)–C(21) is longer than C(sp²)=NR double bonds [unweighted mean over 75 bond lengths 1.279(8) Å⁴²], N(1)–C(51) is shorter than C(sp³)–NR₂ [unweighted mean over 298 C–N bonds 1.488(13) Å⁴²] and C(41)–C(51) [1.415(10) Å] is longer than C=C double bonds [unweighted mean over 104 C=C bonds in cyclopentene 1.323(13) Å⁴²]. The two S–C bond lengths are 1.642(8) [C(41)] and 1.704(8) Å [C(21)]. The Rh–N(1)–C(21), Rh–N(1)–C(51) and C(21)–N(1)–C(51) bond angles are 125.2(6), 125.0(5) and 109.8(6)°, respectively; relevant angles for

Table 4 Downfield range of the ^1H NMR chemical shifts (ppm from SiMe_4) for compounds **2–4** and $[\text{RhCl}_3(\text{SbPh}_3)]$ **5**. The concentrations were ca. 0.01 mol dm^{-3}

In $(\text{CD}_3)_2\text{SO}$		In $\text{DCON}(\text{CD}_3)_2$		In CDCl_3			
2 ^a	$\text{C}_5\text{H}_4\text{N}_4\text{S}$	2 ^b	$\text{C}_5\text{H}_4\text{N}_4\text{S}$	3	4	$\text{C}_3\text{H}_3\text{NS}$ ^c	5
				9.51 [H(21)] 9.31 [H(22)]	9.45 (H ²)		
8.64 (H ²)	8.36 (H ⁸) 8.16 (H ²)	8.79 (H ²)	8.55 (H ⁸) 8.39 (H ²)	8.59 [H(51)] 8.41 [H(52)]	8.57 (H ⁵)	8.86 (H ²)	
7.68, 7.64 (SbPh ₃)		7.91, 7.87 (SbPh ₃)		7.51, 7.47 (SbPh ₃)	7.87, 7.83 (SbPh ₃)	7.96 (H ⁵) 7.41 (H ⁴)	7.51, 7.47 (SbPh ₃)
7.5–7.2 (SbPh ₃)		7.6–7.3 (SbPh ₃) 7.18 (H ⁸)		7.3–7.1 (SbPh ₃ , H ⁴)	7.4–6.9		7.35–6.90 (SbPh ₃)
7.0–6.7 (Ph)		7.0–6.8 (Ph)		6.9–6.8 (Ph)	6.9–6.7 (Ph)		

^a Values for the *N-trans*-to-Sb isomer **B** are δ 8.58 (H⁸) and 8.31 (H²). ^b Values for isomer **B** are δ 8.74 (H⁸), 8.50 (H²), 8.04 and 8.00 (SbPh₃). ^c The solution contained 0.01 mol dm^{-3} SbPh₃.



the thiazole 2 ring are 124.7(5), 123.1(5) and 109.6(6) $^\circ$. The two thiazole ligands are almost planar, the largest deviation from least-square planes being that of C(42B) [0.08(4) Å]. The metal centre deviates 0.1110(6), 0.2338(6) and 0.2910(6) Å from the least-square planes defined by thiazoles 1, 2 and 2B, respectively.

The triphenylstibine ligand. The Sb–C bond distances average 2.134(6) Å in agreement with the values found for complex **2**. The Rh–Sb–C angles average 117.2(2) $^\circ$ whereas the C–Sb–C angles average 100.7(2) $^\circ$. Related bond angles for other transition metals are very similar: see for example, Os–Sb–C [average 117.8(3) $^\circ$] and C–Sb–C [100.0(3) $^\circ$] of *mer*-[Os^{III}Br₃(SbPh₃)₃]⁴⁶ and Au–Sb–C [117.6(2) $^\circ$] and C–Sb–C [100.3(2) $^\circ$] of [Au^I(SbPh₃)₄]⁺.⁴⁷

Spectroscopy

The ^1H NMR spectrum of complex **3** (0.02 mol dm^{-3} , CDCl_3 ; Table 4) shows two signals at δ 9.51 and 9.31 attributable to the H² proton of thiazole 1 (*trans* to Ph) and thiazole 2 ligands, respectively (δ 8.86 for a mixture of thiazole and SbPh₃ in 2:1 molar ratio). The signals at δ 8.59 and 8.41 come from the H⁵ protons, respectively (δ 7.96, thiazole–SbPh₃). The changes in chemical shifts of H² and H⁵ are about 0.65 and 0.45 ppm for thiazoles 1 and 2 when compared to free thiazole: thus, these signals undergo the same change upon co-ordination and the effect is larger than that found for H_o of py (0.38, *trans* to Ph; 0.0, *cis*) in [Rh^{III}Cl₂Ph(py)₃], H_o of dmpy (0.31; –0.05, *cis*) in [Rh^{III}Cl₂Ph(dmpy)₃], H² (0.38) and H⁶ (0.43 ppm) of 4-methylpyrimidine (mpym) in [Rh^{III}Cl₂Ph(mpym)(py)₃].¹⁹

The H⁴ proton of free thiazole resonates at δ 7.41 and is hidden by the complicated signal of SbPh₃ in the spectrum of thiazole–SbPh₃. Complex **3** shows signals at δ 7.51–7.47 (ca. 3 H), a complicated signal at δ 7.3–7.1 and a multiplet at δ 6.9–6.8

(ca. 5 H). The latter absorption can be assigned to the five protons of Ph, on the basis of the spectra of [Rh^{III}Cl₂Ph(py)₃] and [Rh^{III}Cl₂Ph(dmpy)₃]. The intense pattern around δ 7.2 is due to the protons of the SbPh₃ ligand. On examining the intramolecular contact distances for **3** in the solid state it is evident that there are short (Rh) Cl \cdots H (C) contacts involving the SbPh₃ ligand, *i.e.* Cl(1) \cdots H(6p1) 2.87 and Cl(1) \cdots C(6p1) 3.47 Å. The signal at δ 7.51–7.47 is therefore assigned to the *o*-protons from SbPh₃ in close contact with Cl[–]. It should be noted that the formation of a (N) H \cdots Cl bond causes a downfield shift of the proton by about 6 ppm (in CD_2Cl_2).^{48a} A (C) H \cdots halogen interaction is responsible for a downfield shift larger than 1 ppm from the resonance of (C) H in a $(\text{CD}_3)_2\text{CO}$ solution of [PtIme₂{(pz)₂CHMe-*N,N'*}].^{48b} Large downfield shifts upon hydrogen-bond formation have recently been observed also in polar solvents for platinum(II)–guanine complexes.⁴⁹

Consistent with the hypothesis of deshielding effects of (C) H \cdots Cl interactions is the fact that a signal at δ 7.63 is present in the spectrum of complex **1** (the signals relevant to most of the SbPh₃ protons are in the range δ 7.5–6.9). Further experimental evidence comes from the addition of NBuⁿ₄Cl to a solution of **1** in CDCl_3 . The region of the *o*-protons of SbPh₃ is much influenced, the relevant signals being broadened and shifted slightly downfield. The signals of the *p*- and *m*-protons of SbPh₃ as well as those of the phenyl ligand protons are not significantly altered. It should be noted that the spectrum of [Rh^{III}Cl₃(SbPh₃)₃]¹⁹ (see Table 4) has two relatively intense signals at δ 7.51 and 7.47 which correspond to a total of twelve protons. The presence of a third chloride ion in the co-ordination sphere makes it easier for the H_o atoms of SbPh₃ to participate in H \cdots Cl interactions. The (C) H \cdots Cl interactions of chloride ligands in platinum complexes has previously been investigated in the solid state by neutron diffraction.⁵⁰

The ^1H NMR spectrum of complex **4** has peaks at δ 9.45 (H²), 8.57 (H⁵) and 7.85 (two H atoms from SbPh₃). Other resonances at δ 7.4–6.9 are assigned to SbPh₃ and H⁴ protons.

The ^1H NMR spectrum of [RhCl₂(C₅H₄N₄S)Ph(SbPh₃)]·EtOH **2**·EtOH in [²H₇]dimethylformamide (the solid is practically insoluble in chloroform, alcohol, acetone, benzene and water) has singlets at δ 8.79 (H²) of the *S-trans*-to-Sb isomer **A**,

Table 5 Details of the force field for bonds involving the Rh and Sb atoms

	$R_0/\text{\AA}$	$k_r/\text{kJ \AA}^{-2} \text{ mol}^{-1}$
Rh–Sb	2.53	272.0
Rh–Sb (<i>trans</i> to C)	2.65	251.0
Rh–Cl	2.35	376.6
Rh–Cl (<i>trans</i> to Sb)	2.40	355.6
Rh–N (<i>trans</i> to Ph)	2.25	313.8
Rh–N (<i>trans</i> to Sb)	2.12	355.6
Rh–C	2.03	460.2
Sb–C	2.14	376.6
	$\theta_0/^\circ$	$k_\theta/\text{kJ rad}^{-2} \text{ mol}^{-1}$
Sb–Rh–Cl	90	125.5
Sb–Rh–N (<i>trans</i> to Sb)	180	146.4
Sb–Rh–N (<i>cis</i> to Sb)	90	125.5
Sb–Rh–C	90	188.3
Cl–Rh–Cl	180	125.5
Cl–Rh–C	90	125.5
Cl–Rh–N	90	125.5
C–Rh–N (<i>trans</i> to C)	180	125.5
C–Rh–N (<i>cis</i> to C)	90	125.5
C–Sb–C	109.5	25.1
Rh–Sb–C	109.5	104.6
Sb–C–C	120	41.8
Rh–C–C	120	251.0

see solid-state structures and 7.18 (H⁸). The downfield shift of the signal for H² is 0.40 ppm upon complexation. On the contrary, H⁸ experiences an upfield shift of 1.37 ppm in agreement with a shielding effect from a phenyl-ring current of SbPh₃ [see X-ray crystallography, Fig. 1(a)]. On the basis of the distance of H⁸ from the centre of the ring (average 2.5 Å), the calculated shift from the Johnson and Bovey chart⁵¹ should be not higher than 2.5 ppm. The smaller signals at δ 8.74 and 8.50 are attributable to H⁸ and H² of the *N-trans*-to-Sb isomer, B. Noteworthy are the signals at δ 8.00 and 7.97, and 7.91 and 7.87 which are again consistent with short (Rh) Cl \cdots H (Ph) contacts for B and A, respectively. The spectrum in [2H₆]dimethyl sulfoxide recorded from freshly prepared solutions has a peak at δ 8.64 (H², A) and signals at δ 7.68–7.64 [SbPh₃ protons linked to Cl (Rh)], 7.5–7.2 (*m*- and *p*-protons of SbPh₃), and 7.0–6.7 (phenyl ligand protons); two small singlets occur at δ 8.58 (H⁸, B) and 8.31 (H², B). The signal of H⁸ (A) overlaps with those of SbPh₃ or Ph. Spectra recorded a few minutes after dissolution show major changes in the peak patterns, particularly in the region δ 9.0–8.0.

The IR absorption at 1620 cm⁻¹ in the spectrum of complex 2, attributable to the stretching vibration of C=C and C=N bonds of the purine system,^{52a,b} is blue-shifted by about 10 cm⁻¹ consistent with protonation of the N¹ atom as found in the X-ray diffraction analysis. The band at 1160 cm⁻¹ in the spectrum of free purine-6-thione (stretching of the C–S bond^{52c}) is no longer present in the spectrum of 2, in agreement with Rh–S bond formation. The band at 860 cm⁻¹ in the spectrum of free 1,3-thiazole, attributable to the out-of-plane deformation of the N atom coupled with the stretching vibration of the C–S bond,^{52d} is not present in the spectra of 3 and 4. The spectra of 2–4 have a band at 350 cm⁻¹ attributable to the Rh–Cl stretching vibration.^{52e}

Molecular mechanics

The geometrical parameters obtained for the minimized structures (Table 5) show good agreement with the experimental ones. A stacking interaction between thiazole 1 and a phenyl ring from SbPh₃ exists (contact distances between the atoms of the two rings 3.68–3.42 Å) in the computed model of complex 3. This interaction was not found in the solid state probably owing to the intermolecular contacts. The rigid rotation of thiazole 2 around the Rh–N(2) bond shows two

minima at the same energy ($E_T = 16.19 \text{ kJ mol}^{-1}$) for Cl(1)–Rh–N(2)–C(22) torsion angles of 143 and -37° , respectively. The barriers are larger than 125 kJ mol⁻¹. This suggests an equal probability for the two orientations of thiazole 2 around Rh–N(2) and shows that the disorder for this ligand in the solid state is of a statistical type instead of a thermal one. The energy map obtained for rotation of thiazole 1 around the Rh–N(1) bond has two minima for Cl(1)–Rh–N(1)–C(21) -169 (15.82) and 11° (21.71 kJ mol⁻¹). The absolute minimum has the same geometry as that found in the solid state. Noteworthy, thiazole 1 is not affected by disorder in the solid state. Rotation of SbPh₃ around the Rh–Sb axis both for 2 and 3 is hindered by barriers higher than 125 kJ mol⁻¹.

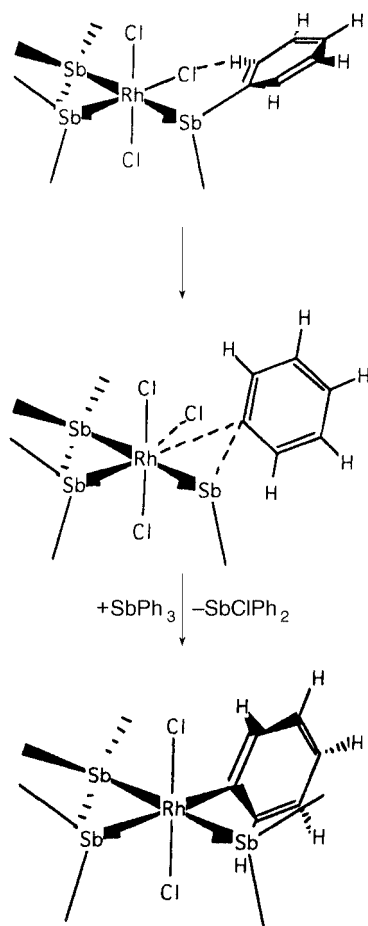
Molecular orbital investigation

The highest occupied molecular orbital (HOMO) has a large contribution from the d_{yz} (complex 2, *ca.* 50%) and d_{xz} (3, *ca.* 40%) atomic orbitals of the metal atoms. The lowest unoccupied molecular orbital (LUMO) consists mainly of the purine atomic orbital for 2 and some atomic orbitals of thiazole and phenyl ligands as well as of phenyl groups of SbPh₃ for 3. The trend of the frontier orbitals is consistent with the splitting, by an octahedral crystal field, of the d orbitals. The HOMO – LUMO gap is about 271.96 and 338.90 kJ mol⁻¹ for 2 and 3, respectively, consistent with a low-spin configuration at room temperature for both compounds. On the basis of Orgel's^{53a} and Griffith's data and formulas,^{53b} pairing energies smaller than 167.36 kJ mol⁻¹ can be estimated for complexed trivalent cations of the second row, far below the computed HOMO – LUMO separation. Noteworthy are the computed 10Dq values for 2 and 3 (510.45 and 514.63 kJ mol⁻¹, respectively) which are similar to the value for [Rh(CN)₆]³⁻ (544.34 kJ mol⁻¹).⁵⁴ The net atomic charges for the chloride ligands of 2 and 3 are $-0.43e$. This value should be compared with the positive charge of 0.04–0.01e computed for the H atoms in the *ortho* positions of the SbPh₃ ligand. The C–H \cdots Cl interactions presented above (see spectroscopy and X-ray crystallography) have therefore also an electrostatic contribution.

An extended-Hückel molecular orbital investigation was carried out with the aim of estimating the energy profile of the formation of [RhCl₂Ph(SbPh₃)₃] 1 from [RhCl₃(SbPh₃)₃]. On the basis of experimental evidence (see also ref. 19, conclusion) the reaction pathway in Scheme 1 is proposed. The products are some 184.10 kJ mol⁻¹ more unstable than the reactants. Obviously, this value is just a rough estimation of the reaction enthalpy, because of the approximation by the theoretical method and the absence of any solvation effects in the model (single-point extended-Hückel energy calculations were carried out for all the molecules). Notwithstanding, it is interesting that, from the reaction of RhCl₃ and SbPh₃ (1:4) in refluxing ethanol and in the absence of Ag⁺, the prevailing species is [RhCl₃(SbPh₃)₃] instead of 1.

In conclusion this work has resulted in the synthesis and structural characterization both in the solid state and in solution of the first complex of Rh^{III} with purine-6-thione; this is stabilized by unusual (C) H \cdots Ph and (C) H \cdots Cl (Rh) interactions. It is the first time, to our knowledge, that a purine H⁸ \cdots Ph interaction has been reported, even though H⁸ \cdots O hydrogen bonds have been previously discussed.⁴³ Similar interactions can be invoked to explain NMR data for DNA-containing systems.⁵⁵ The co-ordination through N⁷ is relatively weak, whereas purine bases usually strongly co-ordinate *via* N⁷.

The synthesis and structural characterization of complexes 3 and 4 show that thiazole is an active ligand for rhodium and that it donates through N instead of S. These facts suggest that the many pharmacologically active molecules¹² containing the



Scheme 1 Systems computed *via* extended-Hückel methods for the analysis of the formation of complex **1**. Just one of the phenyl rings of the SbPh_3 ligands is shown for clarity. The models used in the calculations were $[\text{RhCl}_3(\text{SbH}_3)_2(\text{SbPh}_3)]$, $[\text{RhCl}_2(\text{SbH}_3)_2(\text{SbPh}_2)] \cdots \text{Cl}^- \cdots \text{Ph}^-$, $[\text{RhCl}_2\text{Ph}(\text{SbH}_3)_2(\text{SbPh}_3)]$. Other entities computed were SbPh_3 and SbClPh_2

thiazole moiety can link to Rh^{III} and will hopefully allow the formation and isolation of definite compounds.

Acknowledgements

Financial support from University of Siena, fund 60%, is acknowledged. The X-ray diffraction data collections were carried out at Centro Interdipartimentale di Analisi e Determinazioni Strutturali, University of Siena, with the technical assistance of Mr. Francesco Berrettini.

References

- H. A. O. Hill and J. F. Riordan, *J. Inorg. Biochem.*, 1995, **59**, 183; H. Sigel (Editor), *Metal Ions in Biological Systems*, Marcel Dekker, Basel, 1986, vol. 19; 1983, vol. 16; G. V. Long, M. M. Harding, P. Turner and T. W. Hambley, *J. Chem. Soc., Dalton Trans.*, 1995, 3905.
- See, for example, (a) M. Gielen, *Metal Based Drugs*, 1994, **1**; 1995, **2** and refs. therein; (b) J. Reedijk, *Chem. Commun.*, 1996, 801; (c) P. M. van Vliet, Ph.D. Thesis, University of Leiden, 1996.
- J. R. J. Sorenson, *Prog. Med. Chem.*, 1989, **26**, 437; S. Kirschener, Y. K. Wei, D. Francis and J. G. Bergman, *J. Med. Chem.*, 1969, **9**, 369.
- S. L. Bruhn, J. H. Toney and S. J. Lippard, *Progress in Inorganic Chemistry, Bioinorganic Chemistry*, ed. S. J. Lippard, Wiley, New York, 1990, vol. 38, p. 477.
- L. M. Torres and L. G. Marzilli, *J. Am. Chem. Soc.*, 1984, **106**, 3691.
- K. Aoki, M. Hoshino, T. Okada, H. Yamazaki and H. Sekizawa, *J. Chem. Soc., Chem. Commun.*, 1986, 314.
- K. Aoki and H. Yamazaki, *J. Am. Chem. Soc.*, 1984, **106**, 3691.
- D. P. Smith, E. Kohen, M. F. Maestre and R. H. Fish, *Inorg. Chem.*, 1993, **32**, 4119.
- L. Y. Kuo, M. G. Kanatzidis, M. Sabat, A. L. Tipton and T. J. Marks, *J. Am. Chem. Soc.*, 1991, **113**, 9027.

- A. D. Ryalov, D. L. Menglet and M. D. Levi, *J. Organomet. Chem.*, 1991, **421**, C16.
- M. J. Cleare, in *Recent Results in Cancer Research*, eds. T. A. Connors and J. J. Roberts, Springer, New York, 1974, vol. 48; R. A. Howard, E. Sherwood, A. Erck, A. P. Kimball and J. L. Bear, *J. Med. Chem.*, 1977, **20**, 943; T. Giraldo, G. Sava, G. Bertoli, G. Mestroni and G. Zassinovich, *Cancer Res.*, 1977, **37**, 2662.
- Comprehensive Medicinal Chemistry*, eds. C. Hansch, P. G. Sammes, J. B. Taylor, J. C. Emmett, P. D. Kennewell and C. A. Ramsden, Pergamon, Oxford, 1990.
- S. Kumar, M. Jaseja, J. Zimmermann, B. Yadagiri, R. T. Pon, A.-M. Sapse and J. W. Lown, *J. Biomol. Struct. Dynam.*, 1990, **8**, 99.
- C. Bianchini, *Comments Inorg. Chem.*, 1988, **8**, 27.
- R. T. Baker, D. W. Ovenall and R. Marlow, *Organometallics*, 1990, **9**, 3028.
- E. B. Tjaden and J. M. Stryker, *J. Am. Chem. Soc.*, 1990, **112**, 6420.
- C. S. Chin, S. Y. Shin and C. Lee, *J. Chem. Soc., Dalton Trans.*, 1992, 1323.
- R. S. Hay-Motherwell, S. V. Koschmieder, G. Wilkinson, B. Hussain-Bates and M. B. Hursthouse, *J. Chem. Soc., Dalton Trans.*, 1991, 2821.
- R. Cini, G. Giorgi and L. Pasquini, *Inorg. Chim. Acta*, 1992, **196**, 7.
- G. M. Sheldrick, SHELXL 93, Program for Refinement of Crystal Structures, University of Göttingen, 1993.
- G. M. Sheldrick, SHELXS 86, Program for Crystal Structure Determination, University of Göttingen, 1986.
- M. Nardelli, PARST 95, A System of Computer Routines for Calculating Molecular Parameters from Results of Crystal Structure Analysis, University of Parma, 1995.
- International Tables for X-Ray Crystallography*, Kynoch Press, Birmingham, 1974, vol. 4.
- G. Calzaferri and M. Brändle, ICONC&INPUTC, University of Berne, 1992.
- W. C. Still, F. Mohammadi, N. G. J. Richards, W. C. Guida, M. Lipton, G. Chang, T. Hendrickson, F. DeGunst and W. Hasel, MACROMODEL, version 3.0, Department of Chemistry, Columbia University, New York, 1990.
- S. J. Weiner, P. A. Kollman, D. T. Nguyen and D. A. Case, *J. Comput. Chem.*, 1986, **7**, 230; S. J. Weiner, P. A. Kollman, D. A. Case, U. C. Singh, C. Ghio, G. Alagona, S. Profeta, jun. and P. Weiner, *J. Am. Chem. Soc.*, 1984, **106**, 765.
- R. Cini, R. Pogni, R. Basosi, A. Donati, C. Rossi, L. Sabadini, L. Rollo, S. Lorenzini, R. Gelli and R. Marcolongo, *Metal Based Drugs*, 1995, **2**, 43.
- R. Cini, G. Giorgi and E. Periccioli, *Acta Crystallogr., Sect. C*, 1991, **47**, 716.
- R. Ma, Y.-J. Li, J. A. Muir and M. M. Muir, *Acta Crystallogr., Sect. C*, 1993, **49**, 89.
- K. R. Acharya, S. S. Tavale and T. N. Guru Row, *Acta Crystallogr., Sect. C*, 1984, **40**, 1327.
- F. A. Cotton, K. R. Dunbar, C. T. Eagle, L. R. Falvello, S.-J. Kang, A. C. Price and M. C. Verbruggen, *Inorg. Chim. Acta*, 1991, **184**, 35.
- C. Frei, A. Zilian, A. Raselli, H. U. Güdel and H.-B. Bürgi, *Inorg. Chem.*, 1992, **31**, 4766.
- U. Maeder, A. von Zelewsky and H. Stoeckli-Evans, *Helv. Chim. Acta*, 1992, **75**, 1320.
- R. Cini, A. Cinquantini, M. Sabat and L. G. Marzilli, *Inorg. Chem.*, 1985, **24**, 3903.
- R. Cini, R. Bozzi, A. Karaulov, M. B. Hursthouse, A. Calafat and L. G. Marzilli, *J. Chem. Soc., Chem. Commun.*, 1993, 899.
- A. Zilian, U. Maeder, A. von Zelewsky and H. U. Güdel, *J. Am. Chem. Soc.*, 1989, **111**, 3855.
- M. M. Muir, G. M. Gomez, J. A. Muir and S. Sanchez, *Acta Crystallogr., Sect. C*, 1987, **43**, 839.
- H. I. Heitner and S. J. Lippard, *Inorg. Chem.*, 1974, **13**, 815.
- P. Lavertue, J. Hubert and A. L. Beauchamp, *Inorg. Chem.*, 1976, **15**, 322.
- C. Singh, *Acta Crystallogr.*, 1965, **19**, 861.
- (a) K. Yamanari, M. Kida, M. Yamamoto, T. Fujihara, A. Fuyuhiko and S. Kaizaki, *J. Chem. Soc., Dalton Trans.*, 1996, 305; (b) E. Dubler and E. Gyr, *Inorg. Chem.*, 1988, **27**, 1466.
- F. H. Allen, O. Kennard, D. G. Watson, L. Branner and A. G. Orpen, *J. Chem. Soc., Perkin Trans. 2*, 1987, S1.
- W. Saenger, *Principles of Nucleic Acid Structure*, Springer, Heidelberg, 1984, p. 80.
- N. R. Champness, W. Levason and M. Webster, *Inorg. Chim. Acta*, 1993, **208**, 189.
- G. J. Lamprecht, J. G. Leipoldt and C. P. van Biljon, *Inorg. Chim. Acta*, 1984, **88**, 55.
- C. C. Hincley, M. Matusz and P. D. Robinson, *Acta Crystallogr., Sect. C*, 1988, **44**, 1829.
- P. G. Jones, *Acta Crystallogr., Sect. C*, 1992, **48**, 1487.

- 48 (a) E. Ceci, R. Cini, J. Konopa, L. Maresca and G. Natile, *Inorg. Chem.*, 1996, **35**, 876; (b) P. K. Byers, A. J. Canty, R. T. Honeyman, B. W. Skelton and A. H. White, *J. Organomet. Chem.*, 1992, **433**, 233.
- 49 G. Schröder, B. Lippert, M. Sabat, C. J. L. Lock, R. Faggiani, B. Song and H. Sigel, *J. Chem. Soc., Dalton Trans.*, 1995, 3767.
- 50 L. Brammer, J. M. Chernock, P. L. Goggin, R. J. Goodfellow and A. J. Orpen, *J. Chem. Soc., Dalton Trans.*, 1991, 1789.
- 51 C. E. Johnson, jun. and F. A. Bovey, *J. Chem. Phys.*, 1958, **29**, 1012.
- 52 (a) N. Katsaros and A. Grigoratou, *J. Inorg. Biochem.*, 1985, **25**, 131; (b) N. Kottmair and W. Beck, *Inorg. Chim. Acta*, 1979, **34**, 137; (c) L. J. Bellamy, *The Infrared Spectra of Complex Molecules*, Chapman and Hall, London, 1975, vol. 1; (d) M. M. Muir, M. E. Cadiz and A. Balz, *Inorg. Chim. Acta*, 1988, **151**, 209; (e) K. Nakamoto, *Infrared and Raman Spectra of Inorganic and Coordination Compounds*, Wiley, New York, 1978.
- 53 (a) L. E. Orgel, *J. Chem. Phys.*, 1955, **23**, 1819; (b) J. S. Griffith, *J. Inorg. Nucl. Chem.*, 1956, **2**, 1, 229.
- 54 C. K. Jørgensen, *Absorption Spectra and Chemical Bonding in Complexes*, Pergamon, New York, 1962.
- 55 L. G. Marzilli, personal communication.

Received 25th September 1996; Paper 6/06590B